Optics Communications 426 (2018) 251–256

Contents lists available at ScienceDirect

Optics Communications

journal homepage: www.elsevier.com/locate/optcom

Variable optical attenuator and modulator based on a graphene plasmonic gap waveguide

Feng Chao Ni [a], Ze Tao Xie [a], Qi Chang Ma [a], Jin Tao [c], Lin Wu [c], Changyuan Yu [d], Xu Guang Huang [a,b,*]

[a] Guangzhou Key Laboratory for Special Fiber Photonic Devices and Applications, South China Normal University, Guangzhou 510006, People's Republic of China
[b] Provincial Key Laboratory of Nanophotonic Functional Materials and Devices, South China Normal University, Guangzhou 510006, People's Republic of China
[c] State Key Laboratory of Optical Communication Technologies and Networks, Wuhan Research Institute of Posts & Telecommunications, Wuhan 430074, People's Republic of China
[d] Department of Electronic and Information Engineering, The Hong Kong Polytechnic University, Hung Hom, Kowloon, Hong Kong

ARTICLE INFO

Keywords:
Surface plasmons
Waveguide
Graphene
Integrated optics devices

ABSTRACT

Variable optical attenuation and optical modulation are essential operations in integrated photonic circuits. A new graphene plasmonic gap waveguide structure, which possesses the functions of variable optical attenuator and modulator, is proposed and numerically investigated. The propagation and attenuation modes of the structure can be realized by tuning the gate-voltage. The result shows that it can achieve great modulation depth per micrometer and the working frequency range of 8 THz or more for the variable optical attenuator and the modulator. It also has the advantages of high tolerance, large attenuation range/ modulation depth, wide bandwidth and high integration without crosstalk, which would be promising for high integrated optical circuits.

1. Introduction

Surface plasmon polaritons (SPPs) are light waves trapped on metal–dielectric interface and interacted to free electrons of the conductor. SPPs have the potential to significantly overcome the diffraction limit due to their ability of restricting the electromagnetic field energy in the nanometer range [1,2]. The unique properties of SPPs can be utilized in making ultracompact photonic devices. During the last decade, a great number of SPPs devices have been proposed and numerically studied in various fields, such as integrated photonic circuits [3–5], photovoltaics [6], and biosensing [7].

Graphene, a two-dimensional monolayer of carbon atoms arranged in a hexagonal lattice, has become an attractive candidate for plasmonic material due to its fantastic optical and electronic properties [8]. Its Fermi level can be tuned relative to the Dirac point by applying static electric field, yielding in a nanosecond time [9,10]. Unique virtues of graphene have opened up new avenues for many applications [11,12]. Notably, graphene has become an absorbing alternative for terahertz and mid-infrared region plasmonic material.

Graphene can support the graphene surface plasmons (GSPs) in the terahertz and mid-infrared region due to its monoatomic thickness and strongly enhanced light–matter interactions [13]. As a combination of graphene and surface plasmons, GSPs have the advantages of SPPs and graphene, such as strong local field enhancement [14] and dynamical tenability [15]. In addition, compared to metallic surface plasmon waves, Graphene surface plasmon waves (GSPW) have longer propagation length in the infrared region [16,17]. So far, series of research projects on GSPs waveguides have been carried out by many research groups. For example, A Vakil et al. [18] firstly proposed a 2D ribbon-like graphene waveguide by only applying a gate voltage distribution of step channel-waveguide-shape on a single graphene surface. J Lao et al. [19] investigated the tunable graphene waveguide which consists of a single graphene sandwiched in media. Based on the gate-voltage-controlled mode-guiding or mode-cutoff mechanism, a modulator and attenuator can be achieved. J Li et al. [20] proposed a non-resonant all-optical plasmonic switch based on graphene nanoribbon waveguide in THz region with ultra-compact size and high speed. JQ Wang et al. [21] proposed a graphene integrated silicon slot-waveguide with strong optical absorption. Their result showed that the structure as a responsivity photodetector can achieve the maximum responsivity of 0.273 AW^{-1} in telecommunication band. A Phatak et al. [22] showed the graphene-on-silicon suspended slot-waveguide possessing attractive properties of strong interaction of propagating light with the graphene layer, and

* Corresponding author.
E-mail address: huangxg@scnu.edu.cn (X.G. Huang).

https://doi.org/10.1016/j.optcom.2018.05.029
Received 30 March 2018; Received in revised form 7 May 2018; Accepted 9 May 2018

proposed Mach–Zehnder interferometer and microring modulators. An ultra-compact spectrometer which uses a monolayer graphene as a surface waveguide was demonstrated by X Wang et al. [23] It formed a Fabry–Pérot cavity and achieved tunable transmitting wavelength control by using electric field. J Wang et al. [24] proposed a grating-coupled Otto configuration consisting of a few graphene layers and a germanium prism, and achieved a sharp and sensitive Fano resonance based on the coupling between the GSPs mode and planar waveguide mode. However, there is no report on graphene plasmonic gap waveguide (GPGW) and its components.

As an essential operation in photonics, optical modulation can modulate information into the fundamental parameters of light (amplitude, frequency, phase, polarization) via applying external voltage, and transmit them in free space or in an optical waveguide. In future optical circuits, integrated, high-speed, and miniaturized optical modulators are indispensable. Modulators based on GSPs have become a research focus in recent years. So far, most of graphene-based modulators have one of the mechanisms: (1) Adjusting the interband or intraband absorption transition of graphene by changing the Fermi level with voltage [25]. (2) Electrical modulation based on the mode index [26]. (3) By tuning the resonant wavelength of plasmonic antennas [27]. However, most of them have narrow working wavelength range, which limits their applications in wavelength-division multiplexing (WDM) systems. A variable optical attenuation (VOA) is a passive device used to reduce the optical power level. For some optical networks, VOA plays a vital role because of its ability to control light power. However, only a few VOAs in terahertz regime, which are not GPGW, have been reported [28].

Optical signal processing in integrated photonic circuits and its applications in optical computing require the ability to control light with voltage or even light. In this paper, we propose and numerically study a new flexible design of modulator/attenuator based on the GPGW structure. By tuning the Fermi level of graphene with gate-voltage, GSPs can propagate along the edge of the graphene or diffuse into the interior of graphene, corresponding to the propagation and attenuation modes of the waveguide. Our study suggests that the proposed structure has the advantages of high fault tolerance, large modulation depth/attenuation range, and wide bandwidth.

2. Design of graphene plasmonic gap waveguide model

Under the condition of random phase approximation, the complex surface conductivity $\sigma(\omega)$ of the graphene dominated by the interband transitions and intraband transitions can be calculated by the Kubo equation [29]. The Fermi level of graphene is determined by the carrier concentration n_g, which can be calculated by $E_f = \hbar v_f (\pi n_g)^{1/2}$ (where v_f is Fermi velocity), carrier concentration $n_g = \varepsilon_0 \varepsilon_d V_g / ed$ (where ε_0 is the permittivity in vacuum, ε_d is the relative permittivity of insulating medium, V_g is the applied voltage, and d is the thickness of insulating medium). The relative permittivity in the plane of graphene is defined as [30]:

$$\varepsilon_g = 1 + \frac{i\sigma(\omega)}{\varepsilon_0 \omega t_g} = -\frac{\sigma_{g,i}}{\varepsilon_0 \omega t_g} + 1 + i\frac{\sigma_{g,r}}{\varepsilon_0 \omega t_g}, \quad (1)$$

where t_g is the thickness of graphene. The real part and the imaginary part of the permittivity can be calculated by $\varepsilon_{g,r} = 1 - \sigma_{g,i}/(\varepsilon_0 \omega t_g)$ and $\varepsilon_{g,i} = \sigma_{g,r}/(\varepsilon_0 \omega t_g)$, respectively. From the equation for $\varepsilon_{g,r}$, it can be seen that the real part of the graphene is permittivity $\varepsilon_{g,r}$ negatively correlated with the imaginary part of its surface conductivity $\sigma_{g,i}$. For $\sigma_{g,i} > 0$, it gives $\varepsilon_{g,r} < 0$, where graphene presents a "metal" state and supports TM mode, just like a metal; For $\sigma_{g,i} < 0$, it gives $\varepsilon_{g,r} > 0$, where graphene presents a "dielectric" state and does not support TM mode, but supports weak TE mode. In our simulation, the graphene is in a "metal" state.

Under the condition of the free space wave vector $k_0 \ll k_{sp}$, the graphene surface plasmons wave vector can be expressed as [31]:

$$k_{sp} = \varepsilon_0 \frac{\varepsilon_1 + \varepsilon_2}{2} \frac{2i\omega}{\sigma(\omega)}, \quad (2)$$

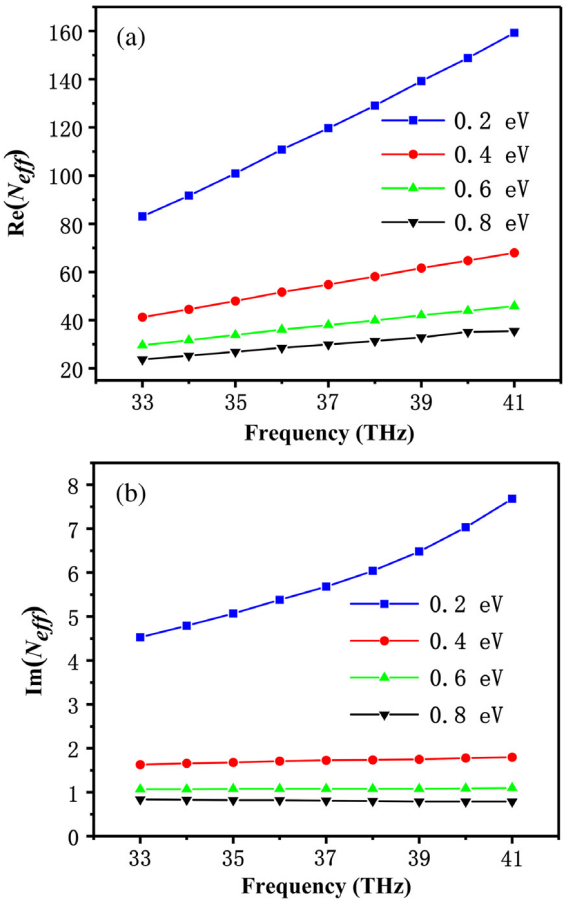

Fig. 1. Variation curves of Re (N_{eff}) (a) and Im(N_{eff}) (b) as the function of frequency for Fermi level E_f = 0.2, 0.4, 0.6, 0.8 eV, respectively.

ε_1 and ε_2 are the relative permittivities of the dielectrics on the top and bottom surfaces of graphene, which are aluminum oxide (Al_2O_3) in this paper. According to the effective index of $N_{eff} = k_{sp}/k_0$ and Eq. (2), the number of N_{eff} can be adjusted by changing the Fermi level of the graphene. Fig. 1(a) and (b) present the variations of Re(N_{eff}) and Im(N_{eff}) of the graphene sandwiched between the two layers of Al_2O_3. In the range of interest, both the real and imaginary parts of the effective index for different E_f increase as frequency goes up, which are more apparent at low Fermi level. It can be explained or understood in Physics or qualitatively as follows. Increasing the Fermi level of graphene means more free electrons being charged and populated in high energy levels of conducting band. Therefore, the conductivity (which is proportional to the number of free electrons) of graphene increases with Fermi level. Based on $N_{eff} = k_{sp}/k_0$ and Eq. (2) (the slope inverse proportional to the conductivity and then inverse correlation to the Fermi level), one can get that the Re(N_{eff}) and Im(N_{eff}) increase as the increase of the frequency with a larger slope at lower Fermi level.

This character can be used to design modulators and variable optical attenuators. The details will be discussed in the next part.

The graphene plasmonic gap waveguide structure is shown in Fig. 2. On the doped silicon substrate, graphene is sandwiched between two Al_2O_3 buffer layers ($H_1 = H_2 = 50$ nm), and is separated into two parts, acting as waveguide cladding sections. The widths of the sandwiched graphene claddings are $W_1 = W_3 = 300$ nm with the width of the central gap of $W_2 = 50$ nm. Moreover, the structure can be highly integrated with multiple waveguides in parallel due to the widths of claddings sections can be only 250 nm.

In the following, the 3D finite-difference time-domain (FDTD) method (Lumerical FDTD solutions software) with perfectly matched

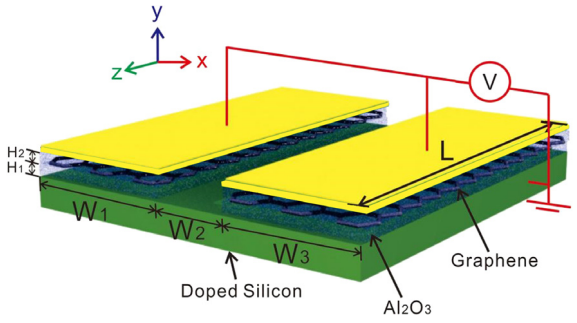

Fig. 2. 3D schematic of the tunable graphene plasmonic waveguide. The width of the gap is $W_2 = 50$ nm, and the widths of the claddings are $W_1 = W_3 = 300$ nm. Graphene is sandwiched between two Al_2O_3 buffer layers with thicknesses of $H_1 = H_2 = 50$ nm. The tops of the waveguide claddings are covered with thin layers of gold as electrodes, and the graphene Fermi level E_f can adjusted by applying an external voltage. The working temperature is $T = 300$ K with graphene relaxation time $\tau = 0.2$ ps. The length L of the structure is set $L = 500$ nm, which can be adjusted as the actual application needs.

layer (PML) absorbing boundary condition is used in simulation to study the optical properties of the waveguide structure. The 2D conductivity model described is used to simulate the optical properties of graphene.

3. Attenuator and modulator based on graphene plasmonic gap waveguide

To demonstrate the tunable optical attenuation characteristics of the waveguide, we simulate the attenuation of the proposed structure with the change of signal light frequency under different Fermi levels of graphene, and the result is shown in Fig. 3(a). One can see that the propagating attenuation of the waveguide gradually increases when the frequency of the signal light raises from 33 THz to 41 THz. The attenuation for $E_f = 0.2$ eV has an obvious variation compared to $E_f = 0.4$, 0.6, 0.8 eV. In addition, 52.26 dB/μm modulation depth can be achieved by adjusting the Fermi level from 0.2 eV to 0.8 eV at 41 THz. The propagating attenuation of the graphene gap waveguide is main determined by the imaginary part $\mathrm{Im}(N_{eff})$ of the graphene cladding, and thus has similar trends as the $\mathrm{Im}(N_{eff})$, Therefore, the attenuation increases with the frequency but decreases with the increase of Fermi level. Fig. 3(b) shows the attenuation of the proposed structure versus the Fermi level at $f = 36$ THz. One can see that the attenuation of the waveguide increases from 5.35 dB/μm to 35.46 dB/μm as E_f decreases from 0.8 eV to 0.2 eV, and thus the modulation depth of 30.11 dB/μm can be achieved. Not only that, it can even realize the attenuation of 129 dB/μm at $E_f = 0.15$ eV, showing a very large attenuation range.

To further investigate the propagating attenuation of GPGW, different Fermi levels of graphene at 36 THz are simulated. From Fig. 4(a), one can see that the GSPW propagates mainly along the edges of the graphene, presenting a relatively low attenuation mode. Comparing Fig. 4(b) with Fig. 4(a), a small portion of GSPW energy diffuses into the graphene cladding, meaning an increase in attenuation, and the result is slightly increased in Fig. 4(c). As E_f decreases to 0.2 eV, an obvious attenuation occurs in Fig. 4(d). The energy of GSPW cannot be concentrated on the graphene edge and diffuses into the graphene cladding, resulting in a large attenuation. Moreover, when the groove width W_2 decreases further, the edge-mode field of the waveguide will spread out into graphene and thus the attenuation of the waveguide will increase severely. Finally, the edge-mode field cannot be supported any more by the gap waveguide, and cut off around $W_2 = 5$ nm, as shown in Fig. 5. Therefore, GSPW will propagate in different attenuation modes when the graphene claddings have different Fermi levels. Based on the above property, the waveguide can be used as a variable optical attenuator (VOA).

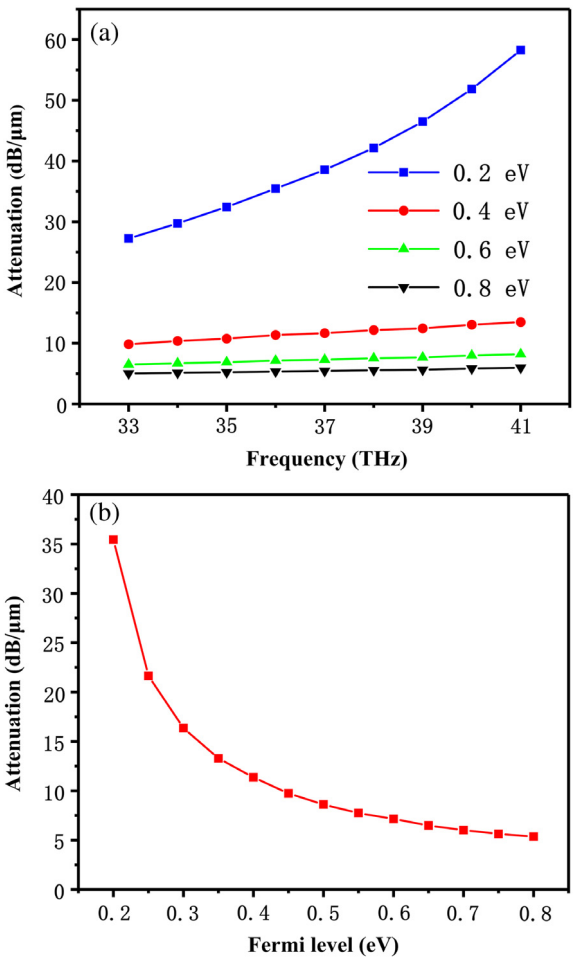

Fig. 3. (a) Curves of attenuation of the waveguide versus frequency for $E_f = 0.2$, 0.4, 0.6 0.8 eV, respectively. (b) The propagating attenuation of the waveguide as the function of the Fermi level of the graphene, at the frequency of the signal light of 36 THz.

As shown in Fig. 6, we also investigate the dependence of the attenuation on big width of the gap. It can be seen that the attenuation of waveguide is nearly invariable. The attenuations for 0.2 eV and 0.8 eV are about 35 dB/μm and 5 dB/μm, respectively. Therefore, the VOA has high fault tolerance and can reduce the precision requirements in actual production.

In addition, we also proposed an optical modulator. Fig. 7 shows the transmission spectra of the waveguide. In the case of $E_f = 0.8$ eV, the transmittance decreases monotonously from 0.56 to 0.5 with the frequency of light from 33 THz to 41 THz; For $E_f = 0.2$ eV, the transmittance decreases from 0.043 at 33 THz to 0.0012 at 41 THz. In addition, the extinction ratio (which are defined as $-10\lg\frac{T_{ON}}{T_{OFF}}$) increases with increasing frequency. The extinction ratio of the modulator is 11.12 dB at 33 THz, while the extinction ratio is 26.22 dB at 41 THz. When the extinction ratio exceeds 10 dB, it can be distinguished to be the "ON" and "OFF" states of the modulator. Therefore, the case of $E_f = 0.8$ eV can be set as the "ON" state of the modulator and $E_f = 0.2$ eV is "OFF" state. Furthermore, the modulator can realize 8 THz optical bandwidth and exhibits broad bandwidth characteristics.

The working bandwidth is indeed one of the most important parameters of optical modulators. It can be estimated with $f_{3\ \mathrm{dB}} = 1/(2\pi\tau_{total})$, here $\tau_{total} = \tau + RC$, τ is the graphene relaxation time, R is the loading resistance, and $C = \varepsilon\varepsilon_0 LW/d$ is the capacitance of the modulator, where $\varepsilon \approx 4.5$ is the relative dielectric constant of insulating medium, and ε_0 is the dielectric constant of vacuum. $L = 500$ nm and $W =$

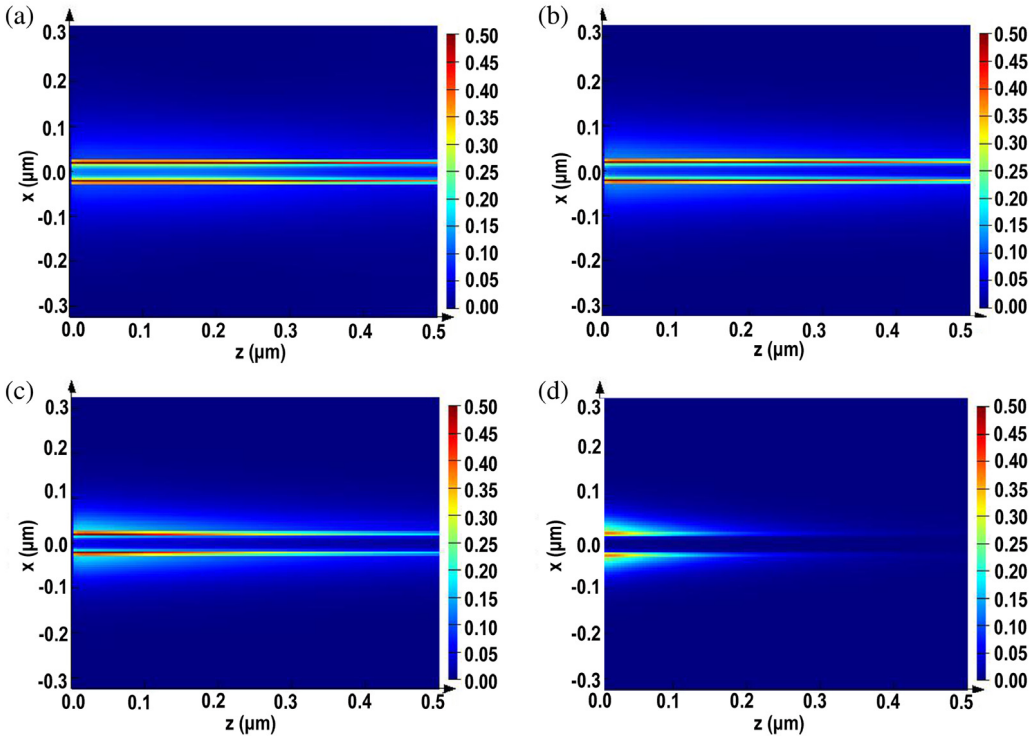

Fig. 4. The $|E|^2$ distributions of the waveguide under different Fermi levels: (a) $E_f = 0.8$ eV, (b) $E_f = 0.6$ eV, (c) $E_f = 0.4$ eV, and (d) $E_f = 0.2$ eV. The frequency of the signal light is at 36 THz.

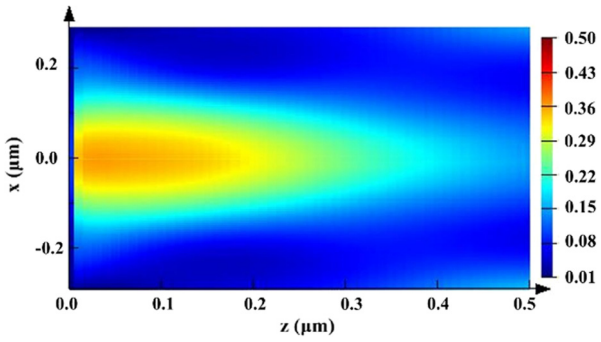

Fig. 5. The $|E|^2$ distribution of the waveguide for $W_2 = 5$ nm and $E_f = 0.8$ eV.

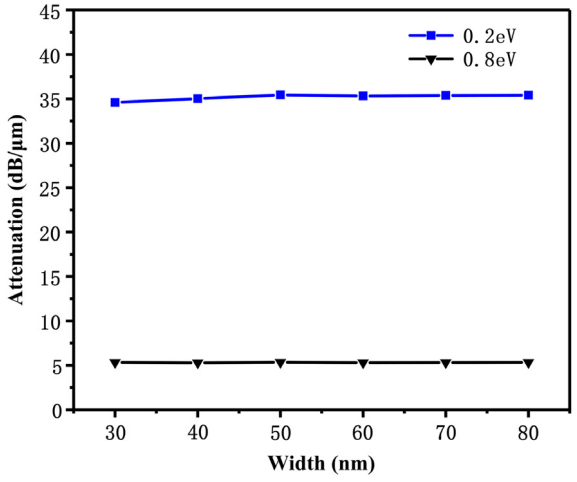

Fig. 6. Attenuation of the waveguide versus the width of the gap at different E_f.

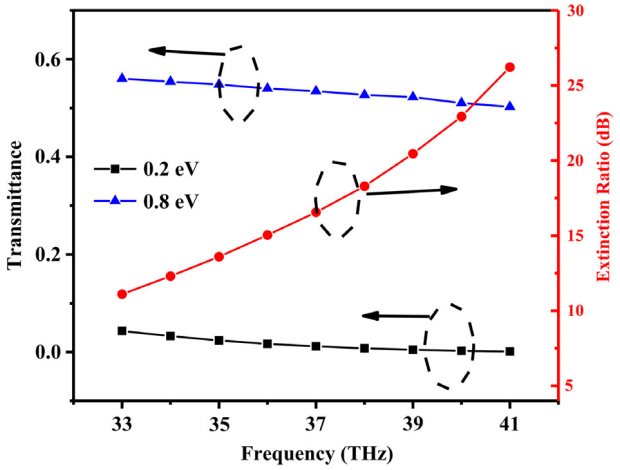

Fig. 7. Transmission spectra and extinction ratio of the modulator waveguide for $E_f = 0.2$ eV and 0.8 eV.

300 nm are respectively the length and width of the electrodes, and $d = 100$ nm is the thickness of insulating medium). For the proposed modulator, the calculated capacitance C is about 0.12 fF. Given a typical loading resistance of $R = 50\ \Omega$, the bandwidth of the modulator can be ~773 GHz, which means the modulator has a very high modulation speed.

Fig. 8 shows the $|E|^2$ distributions of GSPW in the modulator waveguide for "ON" ($E_f = 0.8$ eV) and "OFF" ($E_f = 0.2$ eV) states at 33 THz and 41 THz. When E_f is 0.8 eV at 33 THz, as shown in Fig. 8(a), the GSPW propagates along the boundary between the cladding graphene and the gap of the waveguide, and its energy is mainly concentrated on the edge of the graphene. When $E_f = 0.2$ eV, as shown in Fig. 8(b), some of its energy diffuse into the cladding, resulting in greater loss. Moreover, for a signal light with a frequency of 41 THz under $E_f =$

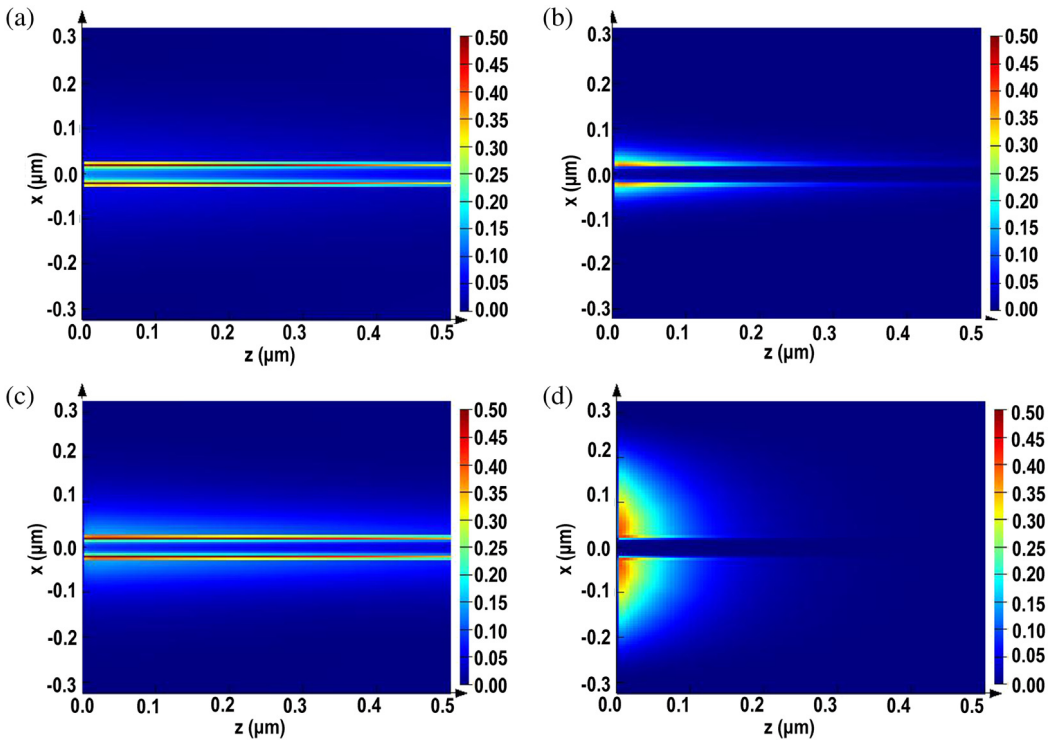

Fig. 8. Propagation profiles of light intensity of the modulator at: (a) and (b) the "on" and "off" states of the modulator at 33 THz, (c) and (d) the "on" and "off" states of the modulator at 41 THz.

0.8 eV, more energy diffuse into the graphene cladding compared to the 33 THz signal light, but still at a relatively low level. When $E_f = 0.2$ eV, most of the energy diffuse into the graphene cladding, and only minimal energy propagates along the boundary, resulting in a great loss. Similar phenomenon happens for the all wavelengths in the range of 33 THz to 41 THz. Based on the above discussion, we can see the effectiveness and broadband modulation characteristics of this modulator.

4. Conclusion

Based on the optical and electronic properties of graphene, we proposed a graphene plasmonic gap waveguide structure. By applying different gate voltage to change the graphene Fermi level, the propagation and attenuation modes of the waveguide can be realized. Additionally, this structure has high width tolerance and high integration. Therefore, we proposed its applications in variable optical attenuator and modulator, which can possess 8 THz bandwidth, and can achieve dynamic attenuation range and large extinction ratio, respectively. This kind of waveguide structure could be used as the basic component of highly-integrated photonic circuits.

Acknowledgments

Natural Science Foundation of China (11674109); Wuhan Morning Light Plan of Youth Science and Technology (2017050304010324); Grant 152113/17E B-Q60D from HK RGC GRF.

References

[1] William L. Barnes, Alain Dereux, Thomas W. Ebbesen, Surface plamons subwavelength optics, Nature 424 (2003) 824–830.
[2] S.I. Bozhevolnyi, V.S. Volkov, E. Devaux, J.Y. Laluet, T.W. Ebbesen, Channel plasmon subwavelength waveguide components including interferometers and ring resonators, Nature 440 (2006) 508–511.
[3] D.K. Gramotnev, S.I. Bozhevolnyi, Plasmonics beyond the diffraction limit, Nat. Photonics 4 (2010) 83–91.
[4] D.K. Gramotnev, M.G. Nielsen, S.J. Tan, M.L. Kurth, S.I. Bozhevolnyi, Gap surface plasmon waveguides with enhanced integration and functionality, Nano. Lett. 12 (2012) 359–363.
[5] J. Tao, Q.J. Wang, B. Hu, Y. Zhang, An all-optical plasmonic limiter based on a nonlinear slow light waveguide, Nanotechnology 23 (2012) 444014.
[6] H.A. Atwater, A. Polman, Plasmonics for improved photovoltaic devices, Nat. Mater. 9 (3) (2010) 205–213.
[7] J.N. Anker, W.P. Hall, O. Lyandres, N.C. Shah, J. Zhao, R.P. Van Duyne, Biosensing with plasmonic nanosensors, Nat. Mater. 7 (2008) 442–453.
[8] A.H. Castro Neto, F. Guinea, N.M.R. Peres, K.S. Novoselov, A.K. Geim, The electronic properties of graphene, Rev. Mod. Phys. 81 (2009) 109.
[9] F. Schwierz, Graphene transistors, Nat. Nanotechnol. 5 (2010) 487–496.
[10] M. Liu, X.B. Yin, E. Ulin-Avila, B.S. Geng, T. Zentgraf, L. Ju, F. Wang, X. Zhang, A graphene-based broadband optical modulator, Nature 474 (2011) 64–67.
[11] J. Tong, M. Muthee, S.Y. Chen, S.K. Yngvesson, J. Yan, Antenna enhanced graphene THz emitter and detector, Nano. Lett. 15 (8) (2015) 5295–5301.
[12] Jin Tao, Lin Wu, Guoxing Zheng, Graphene surface-polariton in-plane Cherenkov radiation, Carbon 133 (2018) 249–253.
[13] F.H.L. Koppens, D.E. Chang, F.J. Garcıa de Abajo, Graphene plasmonics: a platform for strong light–matter interactions, Nano. Lett. 11 (2011) 3370.
[14] V.W. Brar, M.S. Jang, M. Sherrott, J.J. Lopez, H.A. Atwater, Highly confined tunable mid-infrared plasmonics in graphene nanoresonators, Nano. Lett. 13 (6) (2013) 2541–2547.
[15] L. Ju, B. Geng, J. Horng, C. Girit, M. Martin, Z. Hao, H.A. Bechtel, Xi. Liang, A. Zettl, Y.R. Shen, F. Wang, Graphene plasmonics for tunable terahertz metamaterials, Nat. Nanotechnol. 6 (10) (2011) 630–634.
[16] M. Jablan, H. Buljan, M. Soljacic, Plasmonics in graphene at infrared frequencies, Phys. Rev. B 80 (2009) 245435.
[17] J. Christensen, A. Manjavacas, S. Thongrattanasiri, F.H.L. Koppens, F.J. García de Abajo, Graphene plasmon waveguiding and hybridization in individual and paired nanoribbons, ACS Nano 6 (2011) 431–440.
[18] A. Vakil, N. Engheta, Transformation optics using graphene, Science 332 (6035) (2011) 1291–1294.
[19] J. Lao, J. Tao, Q.J. Wang, X.G. Huang, Tunable graphene-based plasmonic waveguides: nano modulators and nano attenuators, Laser Photonics Rev. 8 (4) (2014) 569–574.
[20] J. Li, J. Tao, Z.H. Chen, X.G. Huang, All-optical controlling based on nonlinear graphene plasmonic waveguides, Opt. Express 24 (19) (2016) 22169–22176.
[21] Jiaqi Wang, Zhenzhou Cheng, Zefeng Chen, Xi Wan, Bingqing Zhu, Hon Ki Tsang, Chester Shu, Jianbin Xu, High-responsivity graphene-on-silicon slot waveguide photodetectors, Nanoscale 8 (27) (2016) 13206–13211.

[22] Abhijeet Phatak, Zhenzhou Cheng, Changyuan Qin, Keisuke Goda, Design of electro-optic modulators based on graphene-on-silicon slot waveguides, Opt. Lett. 41 (11) (2016) 2501–2504.
[23] Xiaosai Wang, Chen Chen, Liang Pan, Jicheng Wang, A graphene-based Fabry-Pérot spectrometer in mid-infrared region, Sci. Rep. 6 (2016) 32616.
[24] Jicheng Wang, Ci Song, Jing Hang, Zheng-Da Hu, Feng Zhang, Tunable Fano resonance based on grating-coupled and graphene-based Otto configuration, Opt. Express 25 (20) (2017) 23880–23892.
[25] J. Tao, X. Yu, B. Hu, A. Dubrovkin, Q.J. Wang, Graphene-based tunable plasmonic Bragg reflector with a broad bandwidth, Opt. Lett. 39 (2014) 271–274.
[26] Z.L. Lu, W.S. Zhao, Nanoscale electro-optic modulators based on graphene-slot waveguides, J. Opt. Soc. Amer. B 29 (2012) 1490–1496.
[27] R. Hao, W. Du, H.S. Chen, X.F. Jin, L.Z. Yang, E.P. Li, Ultra-compact optical modulator by graphene induced electro-refraction effect, Appl. Phys. Lett. 103 (2013) 061116.
[28] H. Jian-rong, L. Jiu-sheng, Guo-hua, Graphene-based\waveguide terahertz wave attenuator, J. Infrared Millimeter Terahertz Waves Q. J. Infrared Millim Te 37 (7) (2016) 668–675.
[29] L.A. Falkovsky, S.S. Pershoguba, Optical far-infrared properties of a graphene monolayer and multilayer, Phys. Rev. B 76 (2007) 153410.
[30] H. Lu, C. Zeng, Q. Zhang, X. Liu, M.M. Hossain, P. Reineck, M. Gu, Graphene-based active slow surface plasmon polaritons, Sci. Rep. 5 (2015) 8443.
[31] M. Jablan, H. Buljan, M. Soljacic, Plasmonics in graphene at infrared frequencies, Phys. Rev. B 80 (2009) 24543.